ACS APPLIED MATERIALS & INTERFACES

Research Article

www.acsami.org

Stable Ag@Oxides Nanoplates for Surface-Enhanced Raman Spectroscopy of Amino Acids

Peng Du,[†,∥] Lan Ma,[∥,‡] Yinghui Cao,[§] Di Li,[†] Zhenyu Liu,[§] Zhenxin Wang,[‡] and Zaicheng Sun*[,†]

[†]State Key Laboratory of Luminescence and Applications, Changchun Institute of Optics, Fine Mechanics and Physics, Chinese Academy of Sciences, 3888 East Nanhu Road, Changchun, P. R. China

[‡]State Key Laboratory of Electroanalytical Chemistry, Changchun Institute of Applied Chemistry, Chinese Academy of Sciences, 5625 Renmin Street, Changchun 130022, P. R. China

[§]State Key Laboratory of Applied Optics, Changchun Institute of Optics, Fine Mechanics and Physics, Chinese Academy of Sciences, 3888 East Nanhu Road, Changchun, P. R. China

[∥]University of Chinese Academy of Sciences, Beijing 100000, P. R. China

Supporting Information

ABSTRACT: Surface enhancement Raman scattering (SERS) is a powerful technique for detecting low-concentration analytes (chemicals and biochemicals). Herein, a high-performance SERS biosensing system has been created by using highly stable Ag@oxides nanoplates as enhancers. The Ag nanoplates were stabilized by coating a uniform ultrathin layer of oxides (SiO_2 or TiO_2) on the Ag surface through a simple sol−gel route. The thin oxide layer allows the plasmonic property of the original Ag nanoplates to be retained while preventing their contact with external etchants. The oxides provide an excellent platform for binding all kinds of molecules that contain a COOH group in addition to a SH group. We demonstrate that Ag@oxides have high performance with respect to the typical SERS molecule 4-ATP, which contains a typical SH group. Ag@oxides also can be directly employed for the SERS detection of amino acids. The highly stable Ag@oxides nanoplates are believed to hold great promise for fabricating a wide range of biosensors for the detection of many other biomolecules and may also find many interesting opportunities in the fields of biological labeling and imaging.

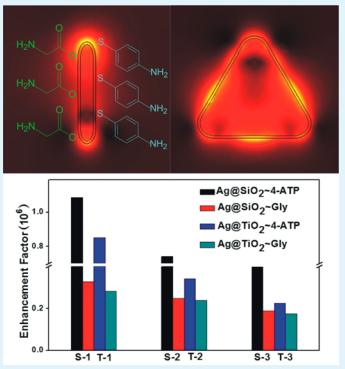

KEYWORDS: *Ag nanoplates, oxides, core−shell nanostructures, SERS, amino acid, plasmonic resonance*

INTRODUCTION

Surface-enhanced Raman spectroscopy (SERS) is a powerful vibrational spectroscopy technique that allows the highly sensitive structural detection of low-concentration analytes (chemicals and biomolecules) through the amplification of electromagnetic fields generated by the excitation of localized surface plasmons.[1−3] SERS is highly dependent on the interaction between adsorbed molecules and the surface of plasmonic nanostructures, often the classic SERS substrates of gold (Au) and silver (Ag).[4−6] Compared with gold, Ag nanostructures produce a much stronger and sharper surface plasmon resonance (SPR) covering a broader spectrum from the ultraviolet (UV) to infrared (IR) region.[7,8] For example, the SPR band of Ag nanoprisms can be tuned from 340 to 1000 nm by changing the size of Ag nanoprisms.[9−11] It has long been recognized that the use of Ag may lead to devices more sensitive than Au.[12]

However, poor chemical and structural stability has been a serious issue, limiting the further practical applications, because the Ag nanostructures tend to evolve into spherical particles, which results in the SPR band blue shift, under acids,[13] halides,[14] oxidants,[15] and heat.[16,17] Therefore, there was a rare report of the SERS application of Ag nanoprisms.[18] Developing strategies for obtaining stable Ag nanostructures while preserving their excellent plasmonic properties for SERS is highly desirable. The typical approach is to modify the surface of the Ag nanostructure with a protecting layer of inorganic or organic materials, such as silica or titania,[19−21] Au,[18,22] and self-assembled monolayers (SAMs) of organic thiols,[23,24] to keep Ag nanostructures away from the external media. Although the stability of protected Ag nanostructure has been improved to some extent, these existing methods are still problematic. For example, it is hard to obtain a Ag@silica core−shell nanostructure with a shell thickness of <15 nm, which limits the use of SERS.[19] Au deposition is initiated at specific sites of Ag nanoparticles, so that the system is stable under mild conditions because of partial Au coverage.[24] Thiol groups oxidize the surface and corner of Ag, thus causing a large decrease in plasmonic activity.[25]

An ideal outer shell layer should provide sufficient protection against disturbance from the environment but should not significantly change the plasmonic property. Herein, we report

Received: March 18, 2014
Accepted: May 18, 2014
Published: May 18, 2014

 © 2014 American Chemical Society

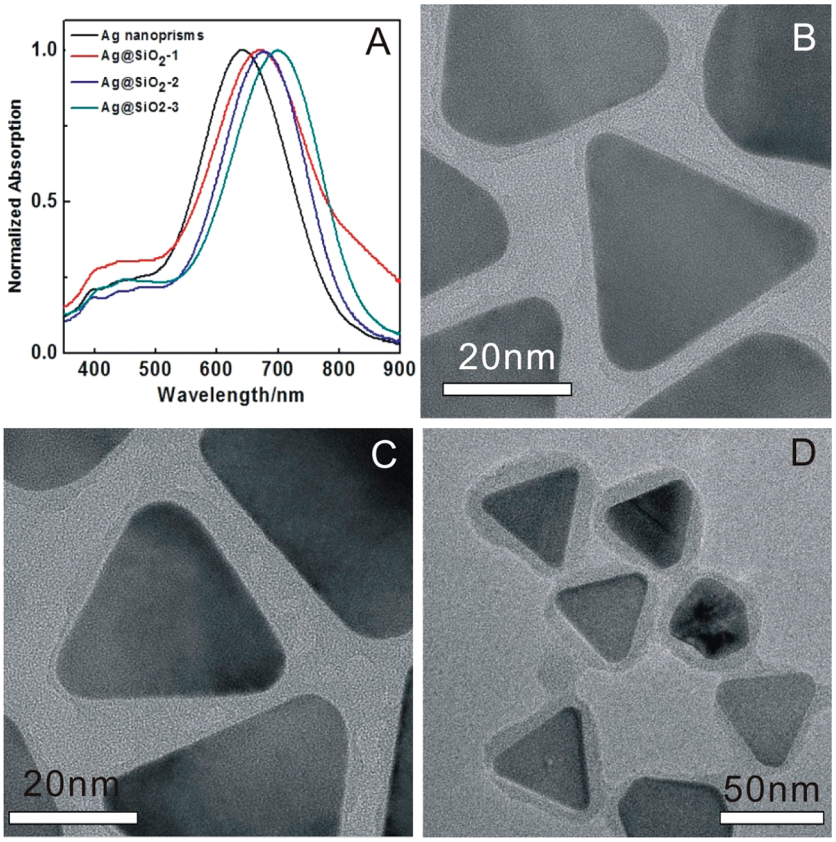

Figure 1. (A) Normalized absorption spectra of the $Ag@SiO_2$ core−shell nanoplates before and after they have been coated with various thicknesses of SiO_2 shells. Transmission electron microscopy (TEM) images of $Ag@SiO_2$ nanoplates with average shell thicknesses of (B) 1.01 ± 0.21, (C) 4.69 ± 1.05, and (D) 8.21 ± 1.39 nm.

a simple sol−gel route for producing highly stable Ag nanoplates with an ultrathin layer of oxides (TiO_2 and SiO_2) and demonstrate their great potential application for SERS sensing of chemicals. Traditionally, the chemicals detected by SERS contain the thiol group, well anchored on the surface of the noble metal nanostructure. The biomolecules without a SH group make it difficult to directly modify the bare surface of metal nanostructures. There have been a few reports of the detection of the molecules without a SH group.[26] However, most biomolecules like amino acids contain a carboxyl group (COOH), which can firmly absorb on the oxide (like SiO_2 or TiO_2) shell of Ag@oxides, which extends the sensor detection range of our Ag@oxides nanoplates.

EXPERIMENTAL SECTION

Chemicals. Poly(sodium styrenesulfonate) (PSSS, 25 wt % solution in water, M_w = 1000000) was purchased from Sigma-Aldrich. Silver nitrate, H_2O_2, NaCl, and *n*-propanol were purchased from Beijing Chemical Co. Tetrabutyl titanate (TBT) (AR grade), tetraethyl orthosilicate (TEOS), sodium citrate, and $NH_3{\cdot}H_2O$ were obtained from Tianjin Guangfu Fine Chemical Research Institute. Sodium borohydride was purchased from Sinopharm Chemical Reagent Co. Ascorbic acid, 4-aminothiophenol (4-ATP), and glycine were purchased from Aladdin Industrial Corp. All the chemicals were used without further purification. Deionized water was purified through a Milli-Q water purification system, and the resistivity was 18.2 MΩ cm.

Synthesis of Ag Nanoprisms. The Ag nanoplates were synthesized using a seed-mediated procedure with a few modifications.[27] First, aqueous sodium citrate (22.5 mL, 2.5 mM), aqueous poly(sodium styrenesulfonate) (PSSS, 2.5 mg), and aqueous $NaBH_4$ (1.5 mL, 10 mM , freshly prepared and cooled at 0 °C) were mixed together successively followed by addition of aqueous $AgNO_3$ (22.5 mL, 0.5 mM) at a rate of 2 mL/min while the mixture was being continuously stirred. Then the yellow solution of Ag seeds was obtained. Second, 45 mL of ultrapure water was mixed with aqueous L-ascorbic acid (0.675 mL, 10 mM) and 1.2 mL of the seed solution, followed by the mixture being dropped into aqueous $AgNO_3$ (27 mL, 0.5 mM) at a rate of 1 mL/min. After that, aqueous trisodium citrate (5 mL, 25 mM) was injected to stabilize the nanoplates. Under magnetic stirring, the color of the solution changed gradually during the dropping of the $AgNO_3$ solution and was finally stable at blue (the peak of the LSPR band at 696 nm). The product was directly used for Ag@oxides core−shell nanoplates without further purification.

Synthesis of $Ag@TiO_2$ Core−Shell Nanoplates. Citric acid (32 mg) was dissolved in 10 mL of *n*-propanol, and then TBT (0.34 g) was added to the citric acid solution. After the mixture had been stirred for 30 min, the TiO_2 sol−gel precursor was filtered with a syringe filter (0.22 μm) for coating Ag nanoplates. The stock Ag nanoplate solution (10 mL) was mixed with 20 μL of 0.7 g/mL aqueous citrate acid, and then 20 μL of the TiO_2 sol−gel precursor was injected while the mixture was being vigorous stirred for 3 h. The thickness of the TiO_2 shell can be tuned by changing the reaction time. Finally, the reaction product was isolated by centrifugation at 10000 rpm for 20 min at 4 °C to remove excessive TiO_2 sol−gel precursor. The precipitate was redispersed in ethanol, and the washing steps were repeated three times to obtain clean $Ag@TiO_2$ nanoplates.

Synthesis of $Ag@SiO_2$ Core−Shell Nanoplates. The SiO_2 sol−gel precursor was obtained by mixing successively ethanol, DI water, $NH_3{\cdot}H_2O$, and tetraethyl orthosilicate (TEOS) in a volume ratio of 184:15:1:0.3. Then, 100 mL of the SiO_2 sol−gel precursor was mixed with 20 mL of a Ag nanoprism solution while the mixture was vigorously stirred for at least 5 h. The thickness of the SiO_2 shell can be tuned by changing the reaction time. Finally, the reaction product

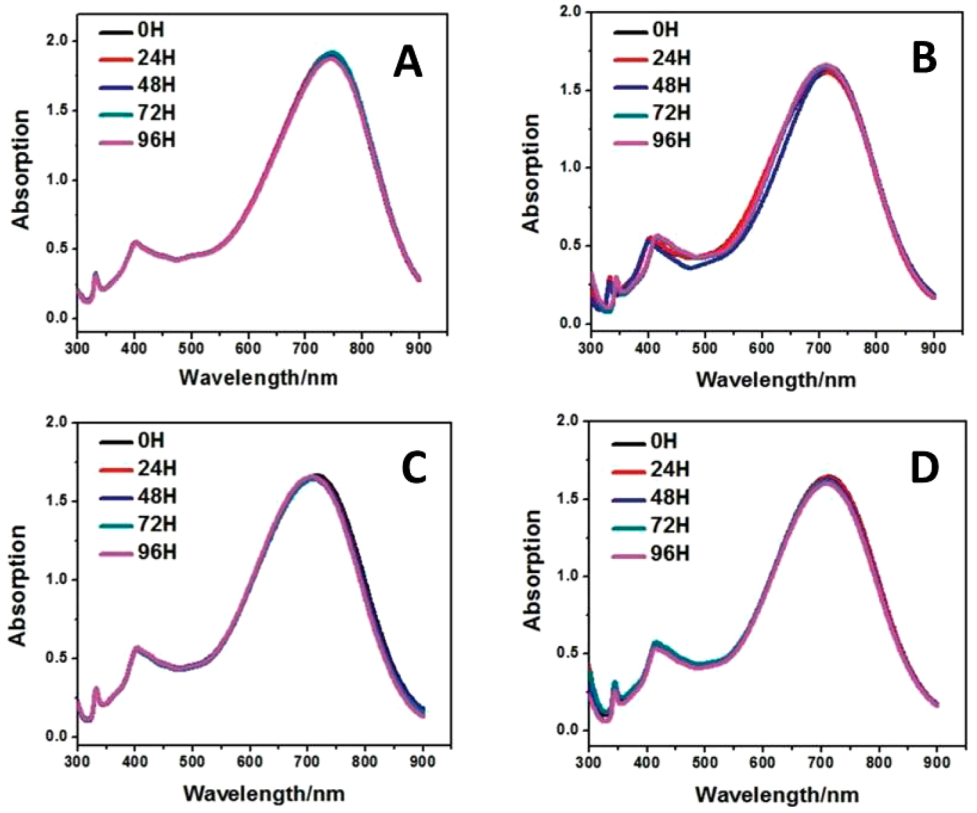

Figure 2. Stability of the $Ag@SiO_2$ nanoplates in (A) H_2O_2 (2.1% aqueous solution), (B) NaCl (20 mM), or (C) PBS (10 mM, pH 7.4, 0.5% PVP) for 96 h. (D) Stability of the $Ag@TiO_2$ nanoplates in H_2O_2 (2.1% aqueous solution) for 96 h.

was isolated by centrifugation at 10000 rpm for 20 min at 4 °C, and the precipitate was redispersed in ethanol. The washing steps were repeated three times to obtain clean $Ag@SiO_2$ nanoplates.

Stability Experiments. A Ag nanoplate, $Ag@TiO_2$ nanoplate, or $Ag@SiO_2$ nanoplate ethanol solution was mixed with H_2O_2 (2.1%), NaCl (20 mM), or phosphate-buffered saline (PBS, 10 mM, pH 7.4, 0.5% PVP) for different periods of time, respectively. Aliquots of the solution were removed at specific times for photographs and UV−vis extinction spectra.

Characterization. The extinction spectra were recorded with a UV−vis absorption spectrometer (Shimadzu UV-2600). Transmission electron microscopy (TEM) images were obtained with a FEI Tecnai G2 transmission electron microscope operating at 200 kV. Scanning electron microscopy (SEM) images of the samples were taken with a field emission scanning electron microscope (JEOL JSM 4800F). Fourier transform infrared (FT-IR) spectra were recorded using KBr pellets with a Bruker Vertex 70 spectrometer from 4000 to 470 cm^{-1}. For surface-enhanced Raman scattering (SERS) measurements, a 20 mg/mL $Ag@TiO_2$ nanoplate or $Ag@SiO_2$ nanoplate ethanol solution was spin-coated at 1000 rpm for 30 s onto the glass substrate as the sample groups, and then a 4-aminothiophenol (glycine) (20 μL, 1 mM) solution in ethanol for 30 min was drop-cast to dry at room temperature, for comparison with the reference substrate of only coating 4-aminothiophenol (glycine) (10 mM, 20 μL). The size of the glass substrate was 1.25 cm × 1.25 cm. Raman spectra were obtained using a Renishaw (Gloucestershire, U.K.) model 2000 spectrometer equipped with an integral microscope (Olympus BX 41). The 514.5 nm radiation from an air-cooled argon ion laser was used as the excitation source. The Raman band of a silicon wafer at 520 cm^{-1} was used to calibrate the spectrometer. SERS spectra were obtained from more than 10 different spots for 5 different samples.

RESULTS AND DISCUSSION

It is known that the plasmonic enhancement of metal nanostructure strongly depends on the distance between the metal surface and adsorbed molecules. Tuning and controlling the thickness of the shell on the Ag nanoplate surface are critical issues in this study. Figure S1 of the Supporting Information shows the SEM image of Ag nanoplates with the SiO_2 shell, indicating that the shape of Ag nanoplates is well maintained after the shell layer has been coated. Figure 1 shows typical TEM images of $Ag@SiO_2$ core−shell nanoplates. The triangular shapes are well retained as expected by the uniform deposition of the SiO_2 shell, for which the shell thickness can be tuned from 1 to 10 nm by changing the reaction time. The plasmonic property is also maintained after coating with SiO_2, as shown via UV−vis spectroscopy (Figure 1A). The plasmonic resonance absorption peak shifts from 641 nm to a long wavelength (671 nm) because of the refractive index change from H_2O to SiO_2. The red shift further increases with an increase in shell thickness. When the SiO_2 layer is ∼8 nm thick, the plasmonic resonance absorption peak shifts to 702 nm. Similar results were also observed in $Ag@TiO_2$ core−shell nanoplates as shown in Figure S2 of the Supporting Information.[20] The red shift of $Ag@TiO_2$ is more significant than that of $Ag@SiO_2$ because TiO_2 has a higher refractive index than SiO_2. Herein, we investigate the effect of Ag nanoplates with different thicknesses of the SiO_2 or TiO_2 shell on the SERS. They were denoted as $Ag@SiO_2$-1, -2, and -3, with shell thicknesses of 1.01 ± 0.21, 4.69 ± 1.05, and 8.21 ± 1.39 nm, respectively. We also investigated $Ag@TiO_2$-1, -2, and -3 core−shell nanoplates, with shell thicknesses of 1.51 ± 0.27, 3.59 ± 2.12, and 7.79 ± 1.58 nm, respectively.

The bare Ag nanoplates are very unstable when they are exposed to different environments. They could be quickly eroded by NaCl, H_2O_2, or PBS (10 mM, pH 7.4, 0.5% PVP), as evidenced by a significant blue shift in the plasmonic resonance

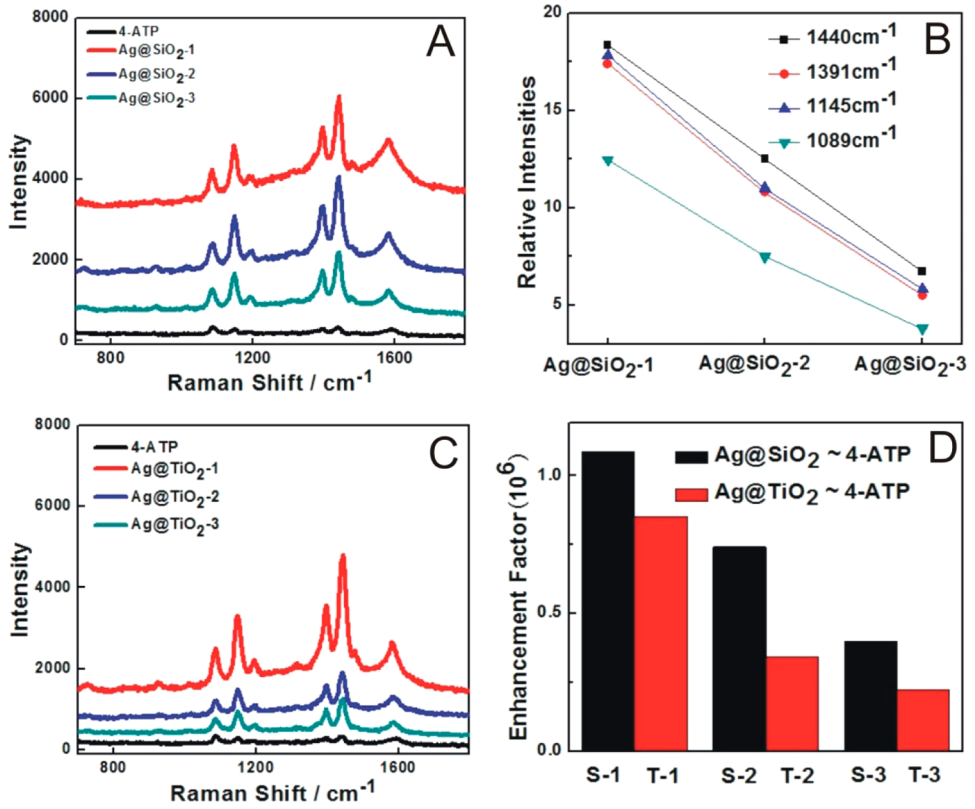

Figure 3. (A) SERS spectra and (B) SERS relative intensities of 4-aminothiophenol (4-ATP) over $Ag@SiO_2$ with different thicknesses of glass substrates. (C) SERS spectra of 4-ATP on $Ag@TiO_2$ with different thicknesses of glass substrates. (D) Enhancement factor (EF) of 4-ATP for Ag@ oxides, where S-1, -2, and -3 stand for $Ag@SiO_2$-1, -2, and -3, respectively, and T-1, -2, and -3 stand for $Ag@TiO_2$-1, -2, and -3, respectively.

absorption peak position and a decrease in the intensity over a relatively short period (Figures S3−S5 of the Supporting Information). The color of the Ag nanoplate solution fades or turns to red in the solution described above, implying that the shape of Ag nanoplates changed in the solutions described above. This is the main reason that original Ag nanoplates have severe limitations in many practical applications in which salts, buffer, or oxidant is present. Even the Ag nanoplates were protected with organic thiols, and their stability was also very limited.[18,23] After the oxides had been coated, the stability of Ag@oxides nanoplates dramatically improved. Figure 2 shows the change in the plasmonic resonance peak of $Ag@SiO_2$, as monitored by UV−vis spectroscopy over time, in NaCl, H_2O_2, or PBS. In all cases, the position and intensity of the plasmonic resonance absorption peak remained unchanged for 96 h, even for the Ag nanoplates with an ultrathin shell (~1 nm). To our surprise, the Ag@oxides are highly stable even in H_2O_2, a strong oxidant that can easily erode the pristine Ag nanoplates within 5 min (Figure S4 of the Supporting Information). They remain unchanged in the case of Ag nanoplates coated with either SiO_2 or TiO_2 shell (Figure 2A,D). The $Ag@TiO_2$ nanoplates also exhibit excellent stability in NaCl and PBS (Figures S6 and S7 of the Supporting Information).

Ag nanoplates coated with oxides are suitable for SERS application. Herein, we first demonstrate the Ag@oxides can be used as SERS-based sensors for a typical model molecule 4-aminothiophenol (4-ATP), because it effectively chemisorbs on the noble metal surface through the SH group. Figure S8 of the Supporting Information presents the FTIR spectra of 4-ATP and 4-ATP on the Ag@oxides. The characteristic peak of the S−H strength vibration is located at 2550 cm^{-1}, which is observed in the FTIR spectrum of 4-ATP. However, this characteristic peak was not observed in the samples of 4-ATP with Ag@oxides. On the other hand, the characteristic peaks of the benzene ring and NH_2 group were present in the samples of 4-ATP with Ag@oxides. These results indicate that the 4-ATP chemisorbed on the surface of Ag@oxides through the SH group. Figure 3A shows SERS spectra of ATP adsorbed on the $Ag@SiO_2$ nanoplates measured with a Raman spectrometer with 514.5 nm excitation and a laser spot of ~0.56 μm^2. The SERS spectra reveal the characteristic peaks of 4-ATP at 1440, 1391, 1145, and 1089 cm^{-1}. The magnitudes of all these SERS signals increased dramatically with the presence of $Ag@SiO_2$ nanoplates on the substrate. The magnitude of the Raman signal is increased ~18-fold for the peak at 1440 cm^{-1} in the case of the Ag nanoplate with an ultrathin SiO_2 shell (1.01 ± 0.21 nm). The relative intensity of characteristic peaks significantly decreased with an increase in shell thickness. The relative intensity of the peak at 1440 cm^{-1} decreased ~8-fold in the case of Ag nanoplates with an ~8 nm thick SiO_2 shell, implying that the SERS signal strongly depends on the distance between the metal surface and adsorbed molecules. Similar results were obtained for the Ag nanoplates with the TiO_2 shell (Figure 3C). It is widely accepted that the SERS effect is the result of enhancement of the localized electromagnetic field due to surface plasmon resonance. As shown in Figure 3B, different relative intensities for peaks at 1440, 1391, 1145, and 1089 cm^{-1} were observed. The relative intensities of peaks at 1440, 1391, and 1145 cm^{-1} are significantly larger than that of the peak at 1089 cm^{-1}. For 4-ATP, Raman peaks at 1440, 1391, and 1145 cm^{-1} are attributed to the benzene ring b_2 mode ($\nu_{CC} + \delta_{CH}$, $\nu_{CH} + \delta_{CC}$ and δ_{CH}, respectively, where ν

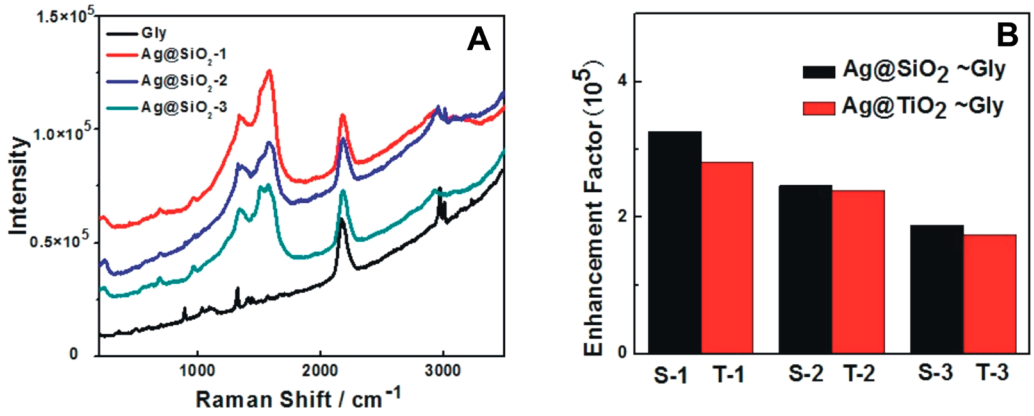

Figure 4. (A) SERS spectra and (B) SERS EF of glycine (Gly) for different thicknesses of Ag@SiO_2 on a glass substrate: S-1, Ag@SiO_2-1; S-2, Ag@SiO_2-2; S-3, Ag@SiO_2-3; T-1, Ag@TiO_2-1; T-2, Ag@TiO_2-2; T-3, Ag@TiO_2-3.

and δ stand for the strength vibration and bending vibration, respectively).[28] The peak at 1089 cm^{-1} is assigned to the a_1 mode (ν_{CS}). According to Han's report,[29] the b_2 modes of 4-ATP on the Ag nanoplate (111) surface exhibit relative intensities stronger than those of the a_1 mode. That indicates most 4-ATP molecules adsorb on the Ag nanoplate (111) plane and the (111) plane tends to be preferentially oriented parallel to the substrate.

The enhancement factor (EF) is a performance indicator of SERS. Qualification of the EF in a SERS substrate needs some assumption because the number of adsorbed molecules is poorly defined.[30] The EF for a SERS system can be described by the equation EF = $(I_{SERS}N_{spot})/(I_{REF}N_{SERS})$, where I_{SERS} is the surface-enhanced Raman intensity, N_{SERS} is the number of molecules bound to the Ag@oxides surface, I_{REF} is the normal Raman intensity of the reference sample, and N_{spot} is the number of molecules in the excitation light spot. In this study, we assume that 4-ATP molecules are uniformly adsorbed in a monolayer on the Ag@oxides nanoplate surface and glass substrate. The EF can be deduced by the equation EF = $(I_{SERS}N_{spot})/(I_{REF}N_{SERS}) = (I_{SERS}A_{spot})/(I_{REF}A_{SERS})$, where A_{SERS} and A_{spot} are the areas of Ag@oxides in the SERS experiment and excitation light spot, respectively. Figure 3D shows the calculated EF for Ag@oxides depending on the shell thickness and shell materials. For the substrates with Ag@SiO_2 nanoplates with an ~1 nm thick shell, the EF is 1.08×10^6. The EF decreases with an increase in shell thickness. The EF is decreased to 3.98×10^5 when the thickness of the SiO_2 shell reaches ~8 nm. When Ag nanoplates are coated with a TiO_2 shell, the EF also decreases to 2.24×10^5 probably because TiO_2 has a higher dielectric constant.

As we known, the carboxyl group can strongly and easily bind on the surface of oxides (SiO_2 and TiO_2). Next, we demonstrate Ag@oxides can be used as a substrate for amino acids, which contain the carboxyl group. Glycine is chosen as a model molecule. Ag nanoplates cannot be directly used for SERS of amino acids because of the instability of Ag nanoplates. Figure S9 of the Supporting Information shows that the color and UV–vis spectra of bare Ag nanoplates changed from blue to cyan within 30 min in the glycine solution, indicating that Ag nanoplates are unstable in the glycine solution. Figure 4 and Figure S10 of the Supporting Information show the SERS of glycine on the bare substrate in the presence of Ag@oxides. The peaks at ~1570 cm^{-1} were significantly enhanced by the presence of Ag@oxides on the substrate. The EF values are 3.27×10^5 and 2.82×10^5 for Ag@SiO_2 and Ag@TiO_2, respectively. These results indicate that Ag@oxides not only could be used for the detection of molecules that contain a SH group but also could be directly used for amino acid or biomolecule detection. There is potential application for the detection of amino acids, protein, and DNA molecules.

CONCLUSIONS

We report a simple sol–gel route for making Ag@oxides core–shell nanoplates with tunable uniform shell thicknesses from 1 to 10 nm. The stability of Ag nanoplates is dramatically improved after they are coated with an ultrathin oxide shell in different solutions, such as NaCl, H_2O_2, and PBS. Generally, the SERS analytes need to contain a SH group or use molecules that contain a SH group as a buffer layer to anchor the analytes on the surface of the noble metal nanostructure surface. We demonstrate that Ag@oxides not only can sense normal molecules that contain a SH group but also can directly detect biomolecules that contain a COOH group such as amino acids, because amino acids tend to self-assemble on the surface of Ag@oxides via the COOH group. That will extend the SERS technique to a large group of biomolecules such as amino acids, DNA, and protein.

ASSOCIATED CONTENT

Supporting Information

Additional SEM, TEM, SERS, and stability data. This material is available free of charge via the Internet at http://pubs.acs.org.

AUTHOR INFORMATION

Corresponding Author

*E-mail: sunzc@ciomp.ac.cn.

Notes

The authors declare no competing financial interest.

ACKNOWLEDGMENTS

We acknowledge financial support from the National Natural Science Foundation of China (21201159, 61176016, and 61306081) and the Science and Technology Department of Jilin Province (20121801). Z.S. is thankful for the support of the "Hundred Talent Program" of the Chinese Academy of Sciences and Innovation and Entrepreneurship Program of Jilin.

REFERENCES

(1) Sharma, B.; Frontiera, R. R.; Henry, A.-I.; Ringe, E.; Van Duyne, R. P. SERS: Materials, Applications, and the Future. *Mater. Today* **2012**, *15*, 16−25.

(2) Kneipp, J.; Kneipp, H.; Kneipp, K. SERS: A Single-Molecule and Nanoscale Tool for Bioanalytics. *Chem. Soc. Rev.* **2008**, *37*, 1052−1060.

(3) Stiles, P. L.; Dieringer, J. A.; Shah, N. C.; Van Duyne, R. P. Surface-Enhanced Raman Spectroscopy. *Annu. Rev. Anal. Chem.* **2008**, *1*, 601−626.

(4) Cho, W. J.; Kim, Y.; Kim, J. K. Ultrahigh-Density Array of Silver Nanoclusters for SERS Substrate with High Sensitivity and Excellent Reproducibility. *ACS Nano* **2012**, *6*, 249−255.

(5) Zhu, Z.; Meng, H.; Liu, W.; Liu, X.; Gong, J.; Qiu, X.; Jiang, L.; Wang, D.; Tang, Z. Superstructures and SERS Properties of Gold Nanocrystals with Different Shapes. *Angew. Chem., Int. Ed.* **2011**, *50*, 1593−1596.

(6) Liu, W.; Zhu, Z.; Deng, K.; Li, Z.; Zhou, Y.; Qiu, H.; Gao, Y.; Che, S.; Tang, Z. Gold Nanorod@Chiral Mesoporous Silica Core−Shell Nanoparticles with Unique Optical Properties. *J. Am. Chem. Soc.* **2013**, *135*, 9659−9664.

(7) Rycenga, M.; Cobley, C. M.; Zeng, J.; Li, W.; Moran, C. H.; Zhang, Q.; Qin, D.; Xia, Y. Controlling the Synthesis and Assembly of Silver Nanostructures for Plasmonic Applications. *Chem. Rev.* **2011**, *111*, 3669−3712.

(8) Xiong, Y.; McLellan, J. M.; Chen, J.; Yin, Y.; Li, Z.-Y.; Xia, Y. Kinetically Controlled Synthesis of Triangular and Hexagonal Nanoplates of Palladium and Their SPR/SERS Properties. *J. Am. Chem. Soc.* **2005**, *127*, 17118−17127.

(9) Yang, Y.; Matsubara, S.; Xiong, L.; Hayakawa, T.; Nogami, M. Solvothermal Synthesis of Multiple Shapes of Silver Nanoparticles and Their SERS Properties. *J. Phys. Chem. C* **2007**, *111*, 9095−9104.

(10) Tiwari, V. S.; Oleg, T.; Darbha, G. K.; Hardy, W.; Singh, J. P.; Ray, P. C. Non-Resonance SERS Effects of Silver Colloids with Different shapes. *Chem. Phys. Lett.* **2007**, *446*, 77−82.

(11) Mulvihill, M. J.; Ling, X. Y.; Henzie, J.; Yang, P. Anisotropic Etching of Silver Nanoparticles for Plasmonic Structures Capable of Single-Particle SERS. *J. Am. Chem. Soc.* **2010**, *132*, 268−274.

(12) Homola, J.; Yee, S. S.; Gauglitz, G. Surface Plasmon Resonance Sensors: Review. *Sens. Actuators, B* **1999**, *54*, 3−15.

(13) Chen, Y.; Wang, C.; Ma, Z.; Su, Z. Controllable Colours and Shapes of Silver Nanostructures Based on pH: Application to Surface-Enhanced Raman Scattering. *Nanotechnology* **2007**, *18*, 325602.

(14) An, J.; Tang, B.; Zheng, X.; Zhou, J.; Dong, F.; Xu, S.; Wang, Y.; Zhao, B.; Xu, W. Sculpturing Effect of Chloride Ions in Shape Transformation from Triangular to Discal Silver Nanoplates. *J. Phys. Chem. C* **2008**, *112*, 15176−15182.

(15) Zhang, Q.; Ge, J.; Pham, T.; Goebl, J.; Hu, Y.; Lu, Z.; Yin, Y. Reconstruction of Silver Nanoplates by UV Irradiation: Tailored Optical Properties and Enhanced Stability. *Angew. Chem., Int. Ed.* **2009**, *48*, 3516−3519.

(16) Tang, B.; An, J.; Zheng, X.; Xu, S.; Li, D.; Zhou, J.; Zhao, B.; Xu, W. Silver Nanodisks with Tunable Size by Heat Aging. *J. Phys. Chem. C* **2008**, *112*, 18361−18367.

(17) Zeng, J.; Roberts, S.; Xia, Y. Nanocrystal-Based Time−Temperature Indicators. *Chem.—Eur. J.* **2010**, *16* (42), 12559−12563.

(18) Gao, C.; Lu, Z.; Liu, Y.; Zhang, Q.; Chi, M.; Cheng, Q.; Yin, Y. Highly Stable Silver Nanoplates for Surface Plasmon Resonance Biosensing. *Angew. Chem., Int. Ed.* **2012**, *51*, 5629−5633.

(19) Xue, C.; Chen, X.; Hurst, S. J.; Mirkin, C. A. Self-Assembled Monolayer Mediated Silica Coating of Silver Triangular Nanoprisms. *Adv. Mater.* **2007**, *19*, 4071−4074.

(20) Du, P.; Cao, Y.; Li, D.; Liu, Z.; Kong, X.; Sun, Z. Synthesis of Thermally Stable Ag@ TiO_2 Core−Shell Nanoprisms and Plasmon-Enhanced Optical Properties for a P3HT Thin Film. *RSC Adv.* **2013**, *3*, 6016−6021.

(21) Li, J. F.; Huang, Y. F.; Ding, Y.; Yang, Z. L.; Li, S. B.; Zhou, X. S.; Fan, F. R.; Zhang, W.; Zhou, Z. Y.; WuDe, Y.; Ren, B.; Wang, Z. L.; Tian, Z. Q. Shell-Isolated Nanoparticle-Enhanced Raman Spectroscopy. *Nature* **2010**, *464*, 392−395.

(22) Shahjamali, M. M.; Bosman, M.; Cao, S.; Huang, X.; Saadat, S.; Martinsson, E.; Aili, D.; Tay, Y. Y.; Liedberg, B.; Loo, S. C. J.; Zhang, H.; Boey, F.; Xue, C. Gold Coating of Silver Nanoprisms. *Adv. Funct. Mater.* **2012**, *22*, 849−854.

(23) Lee, B.-H.; Hsu, M.-S.; Hsu, Y.-C.; Lo, C.-W.; Huang, C.-L. A Facile Method To Obtain Highly Stable Silver Nanoplate Colloids with Desired Surface Plasmon Resonance Wavelengths. *J. Phys. Chem. C* **2010**, *114*, 6222−6227.

(24) Jiang, X.; Zeng, Q.; Yu, A. Thiol-Frozen Shape Evolution of Triangular Silver Nanoplates. *Langmuir* **2007**, *23*, 2218−2223.

(25) Zeng, J.; Tao, J.; Su, D.; Zhu, Y.; Qin, D.; Xia, Y. Selective Sulfuration at the Corner Sites of a Silver Nanocrystal and Its Use in Stabilization of the Shape. *Nano Lett.* **2011**, *11*, 3010−3015.

(26) Selvakannan, P. R.; Ramanathan, R.; Plowman, B. J.; Sabri, Y. M.; Daima, H. K.; O'Mullane, A. P.; Bansal, V.; Bhargava, S. K. Probing the Effect of Charge Transfer Enhancement in off Resonance Mode SERS via Conjugation of the Probe Dye between Silver Nanoparticles and Metal Substrates. *Phys. Chem. Chem. Phys.* **2013**, *15*, 12920−12929.

(27) Aherne, D.; Ledwith, D. M.; Gara, M.; Kelly, J. M. Optical Properties and Growth Aspects of Silver Nanoprisms Produced by a Highly Reproducible and Rapid Synthesis at Room Temperature. *Adv. Funct. Mater.* **2008**, *18*, 2005−2016.

(28) Osawa, M.; Matsuda, N.; Yoshii, K.; Uchida, I. Charge Transfer Resonance Raman Process in Surface-Enhanced Raman Scattering from p-Aminothiophenol Adsorbed on Silver: Herzberg-Teller Contribution. *J. Phys. Chem.* **1994**, *98*, 12702−12707.

(29) Bae, Y.; Kim, N. H.; Kim, M.; Lee, K. Y.; Han, S. W. Anisotropic Assembly of Ag Nanoprisms. *J. Am. Chem. Soc.* **2008**, *130*, 5432−5433.

(30) Le Ru, E. C.; Blackie, E.; Meyer, M.; Etchegoin, P. G. Surface Enhanced Raman Scattering Enhancement Factors: A Comprehensive Study. *J. Phys. Chem. C* **2007**, *111*, 13794−13803.